Quantitative Structural Comparisons of Heme Protein Crystals and Solutions Using Resonance Raman Spectroscopy†

Leyun Zhu, J. Timothy Sage, and Paul M. Champion*

Department of Physics, Northeastern University, Boston, Massachusetts 02115

Received May 6, 1993; Revised Manuscript Received July 26, 1993®

ABSTRACT: Resonance Raman difference spectra have been used to compare crystal and solution samples of metmyoglobin (metMb), deoxymyoglobin (deoxyMb), and cytochrome P450. At pH 6.0, the frequency shifts of the heme core size sensitive bands ν_2, ν_3, and ν_4 were determined to be less than 0.3, 1.0, and 0.3 cm^{-1}, respectively, for metMb and to be less than 1.0, 1.0, and 0.3 cm^{-1}, respectively, for deoxyMb. This shows that the heme core size differences between the crystal and solution conformations are less than 0.002 Å for metMb and less than 0.003 Å for deoxyMb. These results disagree with a recent extended X-ray absorption fine structure study [Zhang, K., Chance, B., Reddy, K. S., Ayene, I., Stern, E. A., & Bunker, G. (1991) *Biochemistry 30,* 9116–9120] which claims that a 0.05-Å difference exists in the average iron–ligand distance between the crystalline and solution forms of metMb at pH 6.5. At pH 8.5, metMb solution samples change gradually from a predominantly high-spin to a predominantly low-spin species as the ammonium sulfate concentration is increased to the level found in the crystal mother liquor. No Raman frequency shifts are found between the crystal and solution forms of metMb at pH 8.5 when the ammonium sulfate concentrations are equal. On the other hand, for deoxyMb, we find a significant alteration in the 220/240-cm^{-1} line shape and relative intensities, suggesting that some histidine–heme perturbation takes place upon crystallization. A continuous-wave photolysis experiment shows that when the MbCO crystal is photolyzed, there is a slow ($\tau \sim 100$ s) increase of the photolyzed population with time. We suggest that this is due to CO moving into the protein matrix of the crystallized protein, leading to long-lived deoxy states, similar to those found in frozen MbCO samples near the glass transition of the solvent.

One of the most important areas of molecular biology is the determination of protein structure and the understanding of its relationship to protein function. Since the pioneering work of Kendrew et al. (1960), X-ray diffraction has become a routine method for the determination of protein crystal structure. However, a question naturally arises concerning whether or not the conditions used to induce crystallization alter the protein conformation. Nuclear magnetic resonance (NMR) techniques for directly determining protein structure in solution are developing rapidly and will ultimately help to resolve this issue. However, this approach is currently limited to proteins of relatively low molecular weight (Wüthrich, 1989). Thus, other high-resolution spectroscopic techniques, which are capable of directly comparing proteins in solution and in single crystals, offer valuable information that can be used to address this question.

For example, resonance Raman studies performed on MbCO[1] single crystals as a function of pH are sensitive to the conformation of the distal pocket (Zhu et al., 1992a) and reveal dynamical differences between crystal and solution samples. Previous work on metMb using Raman spectroscopy has also suggested that a heme propionate group is perturbed in the crystallized protein, but there was no evidence for perturbed iron coordination (Morikis et al., 1988; Sage et al., 1989; Zhu et al., 1992b). In contrast, a recent investigation using extended X-ray absorption fine structure (EXAFS) concluded that significant differences in the Fe coordination shell of metMb are present at pH 6.5 (Zhang et al., 1991a). A more recent EXAFS report (Zhang & Stern, 1993) fails to detect differences at pH 6.2 and thus confirms the original Raman observations. However, the new EXAFS report (Zhang & Stern, 1993) does observe differences between crystal and solution samples at higher pH (~8.5).

Here we report further resonance Raman studies on single crystals of metMb and deoxyMb and make detailed comparisons to solution samples under a variety of conditions. Using Raman difference spectroscopy (Shelnutt et al., 1979), which is very sensitive to small frequency shifts, we are able to quantitatively evaluate the possibility of small changes of the heme geometry in the crystalline and solution environment. In agreement with the recent EXAFS data (Zhang & Stern, 1993), the Raman data indicate apparent crystal/solution differences in metMb crystals at pH 8.5, which we attribute to a high-spin/low-spin transition induced by the ammonium sulfate present in the crystal mother liquor. In addition, we also probe the dynamics of MbCO crystals and find that continuous-wave (cw) photolysis leads to equilibration on a very slow time scale. These latter observations are analogous to previous studies of frozen MbCO solutions near the solvent glass transition (Šrajer et al., 1991) and suggest that the rate of CO migration into the protein matrix is drastically reduced in the crystal.

EXPERIMENTAL PROCEDURES

Lyophilized sperm whale metMb was obtained from Sigma Chemical Co. and was crystallized from ammonium sulfate solutions according to the standard procedure (Kendrew & Parrish, 1956). For the Raman experiments, the monoclinic metMb crystals were mounted on a covered microscope slide or in an X-ray capillary. For experiments at pH 6.0, a 0.1

† This study was supported by grants from NIH (AM-35090) and NSF (90–16860).

® Abstract published in *Advance ACS Abstracts,* September 15, 1993.

[1] Abbreviations: deoxyMb, deoxymyoglobin; metMb, metmyoglobin; MbCO, carbonmonoxymyoglobin; HbCO, carbonmonoxyhemoglobin; NMR, nuclear magnetic resonance; EXAFS, extended X-ray absorption fine structure; cw, continuous wave; OMA, optical multichannel analyzer.

0006-2960/93/0432-11181$04.00/0

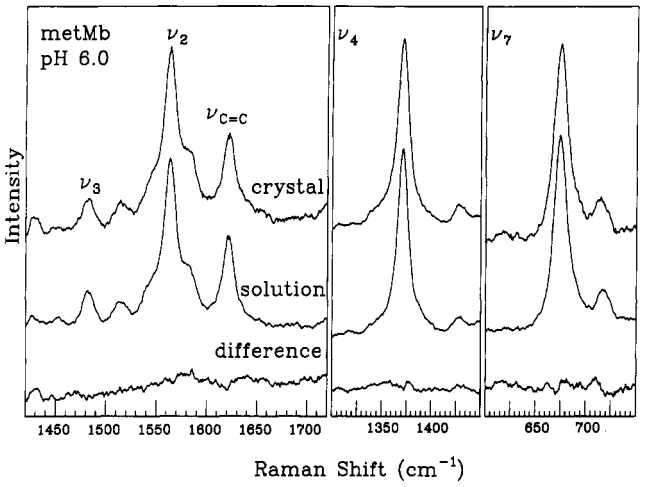

FIGURE 1: Resonance Raman spectra and difference spectra of metMb solution and crystal samples in the high-frequency region. The excitation wavelength is 420 nm. There are no frequency shift features in the difference spectra and the noise level is used to set the upper limit shifts in Table I.

M sodium phosphate buffer was added to the mother liquor. For experiments at pH 8.5, a 0.2 M borate buffer was used and a few drops of sodium hydroxide were added to maintain the pH in the presence of concentrated ammonium sulfate. To form deoxyMb, the vial containing the metMb crystal and mother liquor was flushed with N_2 for 30 min and a small amount of sodium dithionite was added. All the deoxyMb mounting procedures were done in a sealed plastic glove bag filled with N_2 gas. The crystal was inspected using a microscope before and after the experiment to ensure that the crystal was not damaged by mounting or laser illumination. The excitation source was a Coherent CR-699 dye laser with stilbene 3 dye, pumped by a Coherent Innova 100 argon ion laser. The resonance Raman spectra were accumulated with a Spex Triplemate monochromator equipped with 2400 g/mm gratings and a Princeton Instruments optical multichannel analyzer (OMA). For Raman difference spectroscopy, crystal and solution spectra were run back-to-back without changing the optical setup. To ensure accurate difference measurements, both crystal and solution samples were mounted on microscope slides with cover slips, and a back scattering geometry was employed.

For the kinetics experiments, MbCO crystals were prepared as previously described (Zhu et al., 1992a). The crystals were studied at 293 K and at 274 K by flushing with cold nitrogen gas. The laser power was 5 mW, and after adjusting the system to maximize the Raman signal, we blocked the laser beam and translated the MbCO crystal so that the laser would hit a fresh spot when the time-resolved experiment began. After the light was unblocked, the OMA system recorded approximately 300 sequential Raman spectra.

RESULTS AND DISCUSSION

In Figure 1 we show the Raman spectra of crystal and solution samples of metMb, along with their difference spectra. The excitation wavelength is 420 nm, which is near the peak of the Soret band (410 nm). The peak at 1371 cm^{-1} corresponds to ν_4, the porphyrin ring breathing mode (Abe et al., 1978). The peaks at 1564 and 1482 cm^{-1} are the core size sensitive ν_2 and ν_3 modes (Spiro, 1988), while the 1622-cm^{-1} mode is the vinyl C=C stretching mode (Choi et al., 1982). The difference spectra show no frequency shifts between the crystal and solution samples for any of these peaks. The noise in the difference spectra limits the frequency shifts of the ν_4, ν_3, and ν_2 peaks to less than 0.3, 1, and 0.3 cm^{-1}, respectively. Analogous experiments have been carried out on another heme protein, cytochrome P450, with very similar results (Morikis, 1990).

It is well-established from resonance Raman studies of a variety of heme systems that the skeletal modes in the high-frequency region (>1450 cm^{-1}) are correlated with the heme core size as characterized by the porphyrin center to pyrrole nitrogen distance, Ct–N (Spiro, 1988). One can express the mode frequency versus core size by $\nu_i = K_i(A_i - d)$, where ν_i represents the skeletal mode frequency (in reciprocal centimeters), d is the heme core size (Ct–N, in angstroms), and K_i and A_i are mode-dependent constants (Spiro, 1988). This dependence was proposed to be mainly due to changes in the methine bridge bonds as the porphyrin core size changes (Warshel, 1977; Spiro, 1988). Core size correlations for the ν_3, ν_2, and ν_4 frequencies are described using $K = 423.7$, 329.6, and 136.7 cm^{-1}/Å, respectively (Parthasarathi et al., 1987). Accurate frequency measurements are therefore sensitive to changes in the heme core size on the order of 10^{-3} Å. These peaks are also sensitive to the occupancy of the porphyrin π^* orbitals and are therefore quite sensitive to the heme iron spin and oxidation states (Spiro, 1988). As a conservative estimate of the maximum possible frequency shift for ν_2, ν_3, and ν_4, we take the maximum and minimum values of the difference spectrum found in a 30-cm^{-1} window centered on each peak as an upper limit for the difference signal. We then calculate the corresponding frequency shift by the method of Shelnutt et al. (1979), assuming a Lorentzian band shape. Application of the above relationship then limits the core-size differences between metMb solution and crystal to be less than 0.0024, 0.001, and 0.0022 Å, respectively.

Recently, crystal and solution samples of metMb were compared using the extended X-ray absorption fine structure (EXAFS) technique (Zhang et al., 1991a). The central result of that study was the claim that the average iron–nearest neighbor atom distance in the crystalline form is 0.05 Å shorter than in the solution form, and it was proposed that the four Fe–pyrrole nitrogen distances change significantly on going from crystal to solution. Since the Raman analysis limits the heme core size change to less than 0.002 Å, the conclusions based on the EXAFS data suggest that the iron atom must move far away from the heme center. A simple triangulation calculation shows that a 0.05-Å difference in average Fe–N distance would mean that the Fe–Ct distance must change from 0.27 Å (Takano, 1977) to more than 0.56 Å in order to be consistent with the EXAFS analysis. This is even larger than the Fe–Ct distance in the deoxyMb crystal, and a change of this magnitude would inevitably perturb the electron density distribution and induce frequency shifts in the heme Raman spectra. Thus, the Raman data (Morikis et al., 1988; Sage et al., 1989; Zhu et al., 1992b) are in disagreement with the original EXAFS claim (Zhang et al., 1991a) but have evidently been confirmed by more recent EXAFS experiments (Zhang & Stern, 1993).

In the low-frequency region, the spectra of metMb crystal and solution samples are also similar, except for the intensity of the 376-cm^{-1} peak, which is significantly reduced in the crystal and has been previously discussed (Sage et al., 1989). For example, the difference spectrum between crystal and solution limits the shift of the ν_7 band at 675 cm^{-1} to be less than 0.3 cm^{-1}. The other low-frequency peaks have intensity changes and/or poor resolution, making it difficult to determine the upper limits for the frequency shifts. However, no

Table I: Frequency Comparison of Mb Crystals and Solutions at pH 6.0

ν_i	$\Delta\nu_{met}$ (cm^{-1})	$\Delta\nu_{deoxy}$ (cm^{-1})
ν_7	<0.5	<0.3
ν_4	<0.3	<0.3
ν_3	<1.0	<1.0
ν_2	<0.3	<1.0
$\nu_{C=C}$	<0.5	<1.0

obvious frequency shifts were observed in the low-frequency difference spectrum.

The deoxyMb Raman spectrum has a strong ν_4 mode at 1357 cm^{-1}, but the other skeletal and vinyl modes in the high-frequency region have lower intensity in comparison with metMb. When the high-frequency crystal/solution difference spectrum was analyzed for deoxyMb, we again found no frequency shifts. The noise-limited maximum frequency shifts for various peaks of deoxyMb are given in Table I. Upon application of the core-size correlation relationship (Spiro, 1988), we find that the core-size difference between the solution and crystal forms of deoxyMb is less than 0.003 Å.

Figure 2 shows the spectra of solution and crystal forms of deoxyMb and the spectrum of the photolyzed MbCO crystal. The two spectra in the lower part of the figure are excited at 433 nm (the peak of the Soret band). Although no frequency shifts were found, significant relative intensity differences exist in the 220–240-cm^{-1} region. For example, the 243-cm^{-1} mode in the crystal is decreased to the point that it is unresolved from the 220-cm^{-1} mode. The parallel and perpendicular polarized scattering components in the 220–240-cm^{-1} region have been monitored previously (Bangcharoenpaurpong et al., 1984) and in both polarizations the 243-cm^{-1} mode is clearly resolvable from the 220-cm^{-1} mode. This rules out the possibility that the disappearance of the 243-cm^{-1} mode is due to polarization selectivity of the single crystal sample. This difference persists when the excitation wavelength is changed to 420 nm. The top two spectra in Figure 2 are from a photolyzed MbCO crystal and a deoxyMb solution excited at 420 nm. Since 420 nm is the Soret peak position of MbCO, most of the protein is photolyzed, but a small percentage of residual MbCO still shows up in the photoproduct Raman spectra of the crystal. At 420 nm, the cross section of the 252-cm^{-1} mode of MbCO is about 10 times that of the 220-cm^{-1} mode of deoxyMb, while the cross section of the 348-cm^{-1} mode of MbCO is more than 40 times larger than that of the 344-cm^{-1} mode of deoxyMb (Bangcharoenpaurpong et al., 1984; Morikis et al., 1991). We see that, except for the presence of the residual MbCO peaks near 348 and 252 cm^{-1}, the photoproduct spectrum is similar to that of equilibrium deoxyMb. Once again, the intensity of the 243-cm^{-1} mode is significantly reduced (the shoulder near 252 cm^{-1} is due to the presence of a small amount of MbCO).

The 220-cm^{-1} mode of deoxyMb has been assigned as the iron–histidine stretching mode (Kitagawa, 1988; Argade et al., 1984; Wells et al., 1991). The Fe–His mode is sensitive to protein structure, and in the 10-ns photoproduct Raman spectrum of HbCO, it upshifts by about 10 cm^{-1} relative to the equilibrium structure (Friedman, 1985). The fact that no frequency shifts of this mode or the core size indicator modes are observed between crystal and the solution samples of deoxyMb means that the protein environment is similar in both cases. This conclusion does not support the suggestion based on EXAFS measurements that, for deoxyMb in solution, the first coordination sphere of the heme iron atom may contain more than five atoms (Zhang et al., 1991a,b). The ranges of

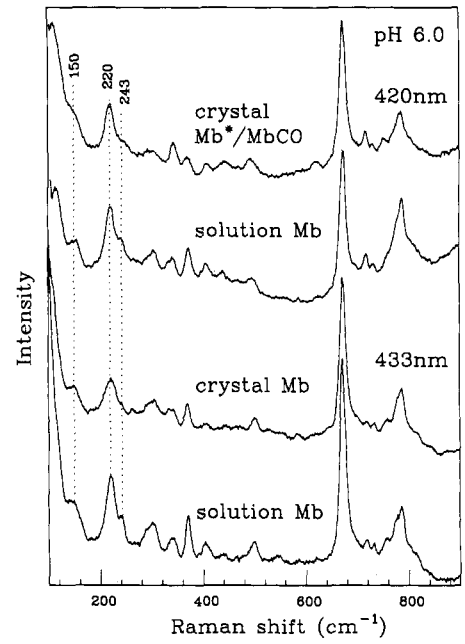

FIGURE 2: Low-frequency resonance Raman spectra of deoxyMb crystal and solution samples along with the crystal MbCO photoproduct Mb*. The excitation wavelengths and sample pH are shown in the figure.

observed frequencies for the core size sensitive modes of five- and six-coordinate hemes do not overlap, and an Fe–His mode is not expected to be present in the spectrum of a six-coordinate heme system. On the other hand, the relative intensity change between the 220- and 243-cm^{-1} modes in the crystalline state indicates that the heme environment is somehow changed by the crystallization process. The 243-cm^{-1} mode has been suggested to be a out-of-plane pyrrole tilting mode on the basis of an isotopic labeling study (Argade et al., 1984), and crystallization evidently alters the coupling of this motion to the π–π^* Soret excitation.

Figure 3 shows the high-frequency spectra of metMb at pH 8.5 in borate buffer with differing amounts of ammonium sulfate. No frequency shifts are detected in the difference spectrum between solution and crystal when the ammonium sulfate concentrations are equal (d and e). The ν_4 shift is less than 0.5 cm^{-1}, while the ν_3, ν_2, and $\nu_{C=C}$ modes show no obvious shifts within the noise (<2 cm^{-1}). As can be seen from spectra a–d, both the intensity and frequency of the peaks depend upon the ammonium sulfate concentration. When the concentration increases from 0% to 80% saturation, ν_4 shifts from 1370 to 1373 cm^{-1}, the 1480-cm^{-1} high-spin ν_3 peak disappears, and the 1511-cm^{-1} low-spin ν_3 peak intensifies and shifts to 1506 cm^{-1}. In addition, the ν_2 peak at 1562 cm^{-1} disappears and reappears at 1577 cm^{-1}, while the $\nu_{C=C}$ peak remains fixed at 1620 cm^{-1} (i.e., shifts less than 1.5 cm^{-1}).

The above results show that there are no significant core size differences (<0.004 Å) between the crystal and solution forms of metMb at pH 8.5 when the ammonium sulfate concentrations are equal. However, the solution spectrum varies with the concentration of ammonium sulfate at pH 8.5 (Figure 3) and both crystal and solution spectra vary with pH at the fixed ammonium sulfate concentration of the mother liquor (e.g., compare Figure 1 and Figure 3e).

The formation of a low-spin complex in metMb crystals at high pH in concentrated ammonium sulfate has been previously noted in single-crystal absorption spectra and attributed to binding of ammonia to the heme iron (Eaton & Hochstrasser, 1968). The shift of the core size sensitive frequencies to values

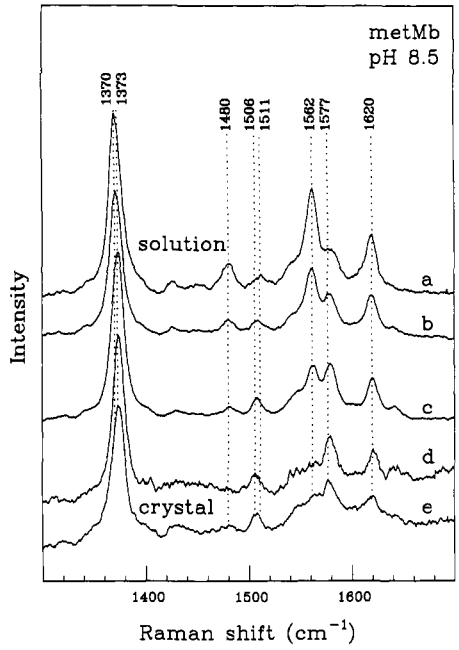

FIGURE 3: Spectra of metMb solution and crystal at pH 8.5. Spectra a–d were recorded for solutions that were 0%, 10%, 40%, and 80% saturated with ammonium sulfate, respectively. The same buffer is used for spectra d and e. The excitation wavelength is 420 nm.

characteristic of a low-spin complex at increased ammonium sulfate concentrations (Figure 3) is consistent with this assignment. These spectral changes are unlikely to be due to the ionization of the heme water ligand to OH^- as recently suggested (Zhang & Stern, 1993), since the Raman spectrum reported for metMbOH^- in the absence of ammonium sulfate (Rousseau et al., 1989) shows both high- and low-spin components, even at pH 11, and is clearly distinct from the fully low-spin spectra observed here at pH 8.5 (Figure 3d,e).

The fact that a high-spin to low-spin transition is observed between pH 6 (Figure 1) and pH 8.5 (Figure 3e) in the crystal or in solution at high ammonium sulfate concentrations (not shown) is also consistent with the binding of ammonia as suggested by Eaton and Hochstrasser (1968). In solutions at pH 6, only the ammonium ion is found in appreciable concentration, and it does not bind to the positively charged ferric heme. However, as the pH is raised, the ammonium ion is titrated to ammonia, which can subsequently bind to the ferric heme creating the low-spin species.

Careful analysis of Figure 3 shows that the low-spin ν_3 peak shifts from 1511 to 1506 cm^{-1} as more low-spin material is formed. From this we infer that the ligand has changed and that the core size of the minority low-spin fraction of metMb is expanded by about 0.012 Å when the (putative) low-spin ammonia bound state is formed. (However, it must be noted that deviations from the core size correlations can appear when the iron ligands are changed.) Obviously, the majority high-spin fraction associated with water ligation undergoes a much larger core size change when ammonia binds and forms a low-spin state.

Figure 4 shows additional experiments that probe the time evolution of the Raman spectra in the ν_4 region after laser irradiation (λ = 420 nm) of the MbCO crystal. When CO is bound (MbCO) the ν_4 band is located at 1373 cm^{-1}, while the ν_4 of the unbound species (deoxyMb) is located at 1351 cm^{-1}. Clearly, the intensity of the deoxyMb peak increases slowly with irradiation time in the crystal. Similar experiments in solution at 293 K approach the photostationary state much more rapidly (on the order of milliseconds or less). The lower

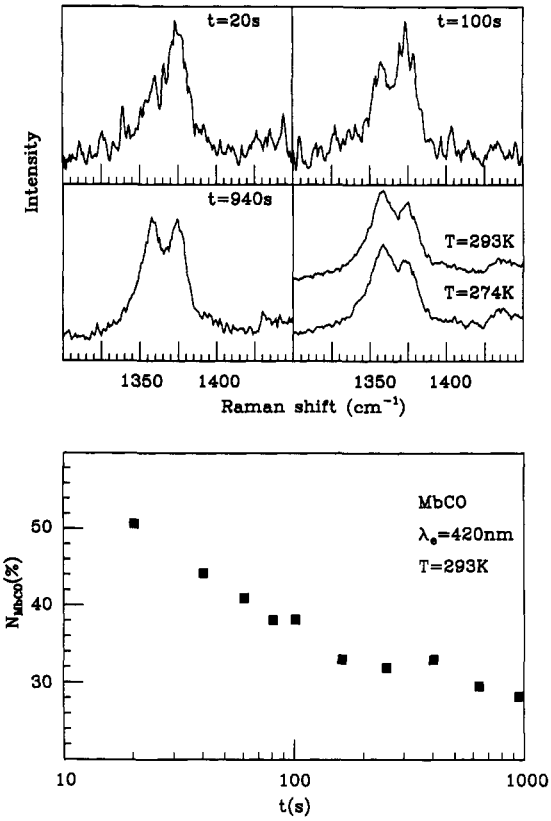

FIGURE 4: The first three windows in the top panel show the Raman spectra recorded at various times after laser illumination is initiated. The fourth window shows the long-time equilibrium spectra at temperatures 293 and 274 K, obtained after several hours of laser illumination. The lower panel shows the corresponding normalized population change of the CO bound species with time. The pH of the samples is 6.0.

part of Figure 4 shows the corresponding population change of MbCO determined using the resonance Raman cross sections of ν_4 at 420 nm (Morikis et al., 1991). [The fitting procedure has been discussed previously by Zhu et al. (1992a).] We see that the time course is highly nonexponential, with decay to photostationary equilibrium taking place between 10 and 10^3 s. The fourth window in the upper panel of Figure 4 shows that the equilibrium populations of MbCO and deoxyMb at 293 and 274 K are nearly the same, demonstrating that small local temperature changes have little effect on the experiments. Thus, the population changes in Figure 4 are associated with a slow time scale ligand migration process that takes place when CO is being photolyzed in the crystal. A similar effect has been noted in studies of frozen MbCO, especially near the "glass" transition at 185 K (Šrajer et al., 1991).

When CO is photolyzed in MbCO crystals, it can either rebind to the heme or move out of the heme pocket into the protein matrix and ultimately escape and diffuse into the mother liquor between the protein macromolecules. Since the protein concentration is much larger than the equilibrium CO concentration in the mother liquor, this latter process could conceivably lead to time-dependent gradients in the local CO concentration that might influence the photostationary state population. However, this phenomenon is ruled out by the following experiment. After illuminating the MbCO crystal for several hours, we block the laser and measure the repopulation of MbCO as a function of time. Since less than one-fifth of the MbCO population returns after 1 h in the dark, we identify the slowly changing Mb/MbCO equilibrium as due to quasi-irreversible CO motion within the protein

matrix of the crystallized sample that leads to the very long-lived deoxyMb states, similar to those observed near the glass transition temperature in 75% glycerol solutions (Šrajer et al., 1991). We note that Iben et al. (1989) also observe a long-lived process in flash photolysis studies of single crystals, which accounts for ca. 10% of the signal amplitude in their experiments. This leads us to propose that the relative motion of CO within (or out of) the crystallized protein takes place on a much slower time scale than for solution samples. This is consistent with previous experiments which demonstrate that the distal pocket interconversions of Mb also take place on a slower time scale in the crystal (Zhu et al., 1992a).

In summary, the Raman analysis shows that no core size difference exists between crystal and solution samples of metMb, at either pH 6.0 or 8.5. However, at pH 8.5, the spin state of the heme iron changes in the presence of concentrated ammonium sulfate, both in the solution and in the crystal samples. This may account for some of the apparent crystal/solution differences derived from the EXAFS experiments. Although the solution and crystal Raman spectra of deoxyMb have a similar structure and core size, small structural differences must exist in order to account for the relative intensity changes of the 220/243-cm^{-1} modes. The dynamics of photolyzed MbCO in the crystal is significantly different than in solution and resembles the behavior previously observed for frozen samples near the glass transition. The fact that ligand escape from the protein matrix and return to the heme are significantly retarded in the crystalline sample suggests that time-resolved X-ray methods might be capable of experimentally determining the ligand trajectory subsequent to photolysis of crystal samples at room temperature.

REFERENCES

Abe, M., Kitagawa, T., & Kyogoku, Y. (1978) *J. Chem. Phys. 69*, 4526–4534.

Argade, P. V., Sassaroli, M., Rousseau, D. L., Inubushi, T., Ikeda-Saito, M., & Lapidot, A. (1984) *J. Am. Chem. Soc. 106*, 6593–6596.

Bangcharoenpaurpong, O., Schomacker, K. T., & Champion, P. M. (1984) *J. Am. Chem. Soc. 106*, 5688–5698.

Choi, S., Spiro, T., Langry, K., & Smith, K. (1982) *J. Am. Chem. Soc. 104*, 4337–4344.

Eaton, W. A., & Hochstrasser, R. M. (1968) *J. Chem. Phys. 49*, 985–995.

Friedman, J. M. (1985) *Science 228*, 1273–1280.

Iben, I. E. T., Keszthelyi, L., Ringe, D., & Varo, G. (1989) *Biophys. J. 56*, 459–463.

Kendrew, J., & Parrish, R. (1956) *Proc. R. Soc. London, A 238*, 305–324.

Kendrew, J., Dickerson, R., Strandberg, B., Hart, R., Davies, D., Phillips, D., & Shore, V. (1960) *Nature 185*, 422–427.

Kitagawa, T. (1988) in *Biological Applications of Raman Spectroscopy* (Spiro, T. G., Ed.) Vol. III, pp 97–131, Wiley-Interscience, New York.

Makinen, M., Houtchens, R., & Caughey, W. (1979) *Proc. Natl. Acad. Sci. U.S.A. 76*, 6042–6046.

Morikis, D. (1990) Ph.D. Thesis. Northeastern University, Boston, MA.

Morikis, D., Li, P., Bangcharoenpaurpong, O., Sage, J. T., & Champion, P. M. (1991) *J. Phys. Chem. 95*, 3391–3398.

Parthasarathi, N., Hansen, C., Yamaguchi, S., & Spiro, T., G. (1987) *J. Am. Chem. Soc. 109*, 3865–3871.

Rousseau, D. L., Ching, Y., Brunori, M., & Giacometti, G. M. (1989) *J. Biol. Chem. 264*, 7878–7881.

Sage, J. T., Morikis, D., & Champion, P. M. (1989) *J. Chem. Phys. 90*, 3015–3032.

Shelnutt, J. A., Rousseau, D. L., Dethmers, J. K., & Margoliash, E. (1979), *Proc. Natl. Acad. Sci. U.S.A. 76*, 3865–3869.

Spiro, T. G., & Li, X. Y. (1988) in *Biological Applications of Raman Spectroscopy* (Spiro, T. G., Ed.) Vol. III, pp 1–37, Wiley-Interscience, New York.

Šrajer, V., Reinisch, L., & Champion, P. M. (1991) *Biochemistry 30*, 4886–4895.

Takano, T. (1977) *J. Mol. Biol. 110*, 537–568.

Warshel, A. (1977) *Annu. Rev. Biophys. Bioeng. 6*, 273–300.

Wells, A. V., Sage, J. T., Morikis, D., Champion, P. M., Chiu, M. L., & Sligar, S. G. (1991) *J. Am. Chem. Soc. 113*, 9655–9660.

Wüthrich, K. (1989) *Acc. Chem. Res. 22*, 36–44.

Zhang, K., Chance, B., Reddy, K. S., Ayene, I., Stern, E. A., & Bunker, G. (1991a) *Biochemistry 30*, 9116–9120.

Zhang, K., Reddy, K. S., Bunker, G., & Chance, B. (1991b) *Proteins: Struct., Funct., Genet. 10*, 279–286.

Zhang, Y., & Stern, E. (1993) *Bull. Am. Phys. Soc. 38*, 267.

Zhu, L., Sage, J. T., Rigos, A. A., Morikis, D., & Champion, P. M. (1992a) *J. Mol. Biol. 224*, 207–215.

Zhu, L., Sage, J. T., & Champion, P. M. (1992b) *Bull. Am. Phys. Soc. 37*, 447.